Microgravity Sci. Technol (2008) 20:73–80
DOI 10.1007/s12217-008-9040-5

Velocity Distribution of Vibration-driven Granular Gas in Knudsen Regime in Microgravity

M. Hou · R. Liu · G. Zhai · Z. Sun · K. Lu · Y. Garrabos · P. Evesque

Received: 5 January 2007 / Accepted: 5 June 2008 / Published online: 3 July 2008

Abstract Dynamics of quasi-2D dissipative granular gas is studied in micro-gravity condition (of the order of 10^{-4} g) in the limit of Knudsen regime. The gas, made of 4 spheres, is confined in a square cell enforced to follow linear sinusoidal vibration in ten different vibration modes. The trajectory of one of the particles is followed for 2 hours, and is reconstructed from video data by particle tracking. From statistical analysis, we find that (i) loss due to wall friction is small, (ii) trajectory looks ergodic in space, and (iii) distribution $\rho(v)$ of speed follows an exponential distribution, i.e., $\rho(v) \approx \exp\left[-v/\left(v_{x_0,y_0}\right)\right]$, with v_{x_0,y_0} being a characteristic velocity along a direction parallel (y) or perpendicular (x) to vibration direction. This law deviates strongly from the Boltzmann distribution of speed in molecular gas. Comparisons of this result with previous measurements in earth environment, and what was found in 3D cell (Falcon et al., Europhys Lett 74:830, 2006) performed in environment of about $\pm 5 \times 10^{-2}$ g are given.

M. Hou (✉) · R. Liu · Z. Sun · K. Lu
Beijing National Laboratory for Condensed Matter Physics, Institute of Physics, Chinese Academy of Sciences, Beijing, 100080 China
e-mail: mayhou@aphy.iphy.ac.cn

G. Zhai · Z. Sun
Center for Space Science and Applied Research, Chinese Academy of Sciences, Beijing, 100080 China

Y. Garrabos
ESEME-ICMCB, UPR 9048 CNRS, Univerité Bordeaux 1, 33608 Pessac, France

P. Evesque
Lab MSSMat, UMR 8579 CNRS, Ecole Centrale Paris, 92295 Chatenay-Malabry, France

Keywords Granular gas · Velocity distribution

Introduction

The behavior of granular matter in micro-gravity has been studied only very recently (Falcon et al. 1999), while it was simulated a little earlier (McNamara and Young 1992) with different kinds of computing programs (Poschell and Luding 2001; Poschel and Brilliantov 2003; Goldhirsch 2003). Despite its fundamental aspect, the acquisition of this knowledge is of major challenge as soon as man will like to stay traveling far from the earth through long term journey because most human activities manipulate grains at some stage.

The first 0 g experiments on granular media were to test essentially $3D$ samples with a small feeding ratio, from 1 grain to a few hundreds, in a cell which was agitated according to sinusoidal mechanical vibration. The physics addressed is that of a gas, which dissipates energy during collisions, and needs continuous excitation so as for the system not to freeze. From the viewpoint of statistical mechanics, this dissipation is not a classic situation, and may produce important changes of behavior compared to the classic gas of molecules. Indeed, these micro-gravity experiments have produced quite non classic behaviors (Falcon et al. 2006, 1999; Leconte et al. 2006a), which were not predicted by simulation or by theory (Poschell and Luding 2001; Poschel and Brilliantov 2003; Goldhirsch 2003; Barrat et al. 2005). For instance two of them particularly interest us in the present paper: (i) the non ergodic behaviour of the dissipative-billiard played with 1 or 2 balls (Evesque et al. 2005; Leconte et al. 2006b), for which one has

found periodic bouncing solutions with an important reduction of the efficient phase space (from $13d$ to $1d$); (ii) non classic distribution of speed of a dilute gas system (Falcon et al. 2006) when the mean free path l_c of the particle becomes of the order of the cell size. A non-Boltzmann speed distribution at impact with the immobile wall is found. It instead follows $\exp\left[-v/v_0\right]$ law with v_0 proportional to the typical piston speed $b\omega$ and scales as $N^{-0.4}$(Falcon et al. 2006; Evesque 2004), where N is the total number of balls.

In this paper, we pursue this investigation with the case of a quasi-$2D$ dissipative gas in a low density regime and excited by linearly polarized sinusoidal shaking in microgravity (of the order of 10^{-4} g). Movement of one particle in a cell of four moving particles is video recorded for 2 hours in ten different vibration modes. The particle trajectory is traced and analyzed, and its velocity distribution is drawn for each vibration mode. We expect a velocity distribution close to Maxwell-Boltzmann distribution, $\exp\left[-v^2/(kT)\right]$, as in gas phase. It is, however, found that the velocity distribution in either x or y direction is an exponential function of $\left(-v_{x,y}/v_{x_0,y_0}\right)$, where v_{x_0,y_0} is characteristic velocity along x or y direction, which is linearly proportional to the maximum vibration velocity v_b $(=b\omega$, where b is the vibration amplitude and ω is the angular velocity of the cell).

Simulations (Losert et al. 1999) and experimental studies (Brey and Ruiz-Montero 2003; Moon et al. 2004) published so far find the velocity distributions of granular gases are of the form $\exp\left(-\left(\frac{v}{v_0}\right)^{\alpha}\right)$ with α varies from 1 to 2 depending on the restitution coefficient of particles, the friction of particles with the cell walls, the number of particles in the system, and if rotation and gravity are taken into consideration. In our case the experiments are performed in microgravity, friction caused by the lateral walls is not significant, and although the only attaching force is given by the vibrating wall in y direction, particle motions seem ergodic that they occupy randomly all the accessible area in the cell. Presumably one would expect a velocity distribution closer to Gaussian that α is closer to 2. Our experimental findings, however, show a velocity distribution with a value of $\alpha \approx 1$. This exponential dependence is similar to what is obtained previously in $3D$ cell (Falcon et al. 2006) in Knudsen regime in parabolic flight experiments, although different by a factor of $1/v$.

Experimental Process

The experiment was carried out in Satellite SJ-8 launched in September 2006. The square cell (1 cm^2) is filled with four freely moving bronze spheres (diameter $d = 1.21 \pm 0.02mm$) and four others, which are glued along the bottom side near the right corner so that the cell shape can not be considered as a square. The four side walls of the cell are in bronze, and the cell is closed by two sapphire windows that allows lighting, viewing and video recording and which are separated by $\delta = d + 0.1\ mm = 1.31 \pm 0.02\ mm$ so that ball rotation is allowed in the three directions, while translation motion of freely moving balls is essentially $2d$.

This cell is part of a group of 14 cells (Fig. 1b) mounted on a translating carrier which is activated by a model 57000 electric hybrid linear actuator from Haydon Switch & Instrument INC. The amplitude and frequency of vibration can be adjusted via a home-made controller card. This group of 14 cells is subdivided into four sets (labeled A,B,C,D from left to right and top to bottom) of equivalent size (see Fig. 1b), containing respectively 2, 4, 4 and 4 cells. The cell which interests us is the cell located at the bottom right corner of group C (Fig. 1b).

The complete setup is contained in a 30 cm × 30 cm × 40 cm aluminum box located in the non recoverable part of SJ-8. Top view of the apparatus is shown in Fig. 1(a), where parts and cards are located. The box contains the cell carrier coupled to the vibrator, 4 CCD cameras and their optics (one for each sub-group of cells), 2 white LEDs to enlighten the cells, and necessary electronics: a home-made vibrator-controller card, a power supply card for the vibrator and an image-by-image video compression card. The compressed image sequences are stored in the central unit of SJ-8, then sent to earth.

The system works as follows: The vibration is imposed by the vibrator at the amplitude and frequency $f = \omega/(2\pi)$ pre-programmed in the home-made controller card; each mode lasts for a duration T, parameters are then changed automatically, i.e., the controller is pre-coded to impose the series of parameters $(b_k, f_k, T_k,)$. The two white light LEDs, one on each side of the cell holder, are used as front light sources. The images of the particles are recorded by 4 (Watec 231S) CCD cameras with PAL standard (752 × 582 *pixels*) resolution, 25 *frames/s*). Optics imposes that 1 *pixel* = 0.112 *mm*. The image signals are compressed via a home-made card with a compression rate of 8:1 and transmitted in sequence to be stored in a hard disk, then tele-transmitted to earth. The compressed video data are recoverable after the satellite returns. A position sensor is fixed on the carrier to measure the amplitude and frequency of vibration.

The experiment lasts for 2 hours, during which 10 modes of linear vibration have been applied; their

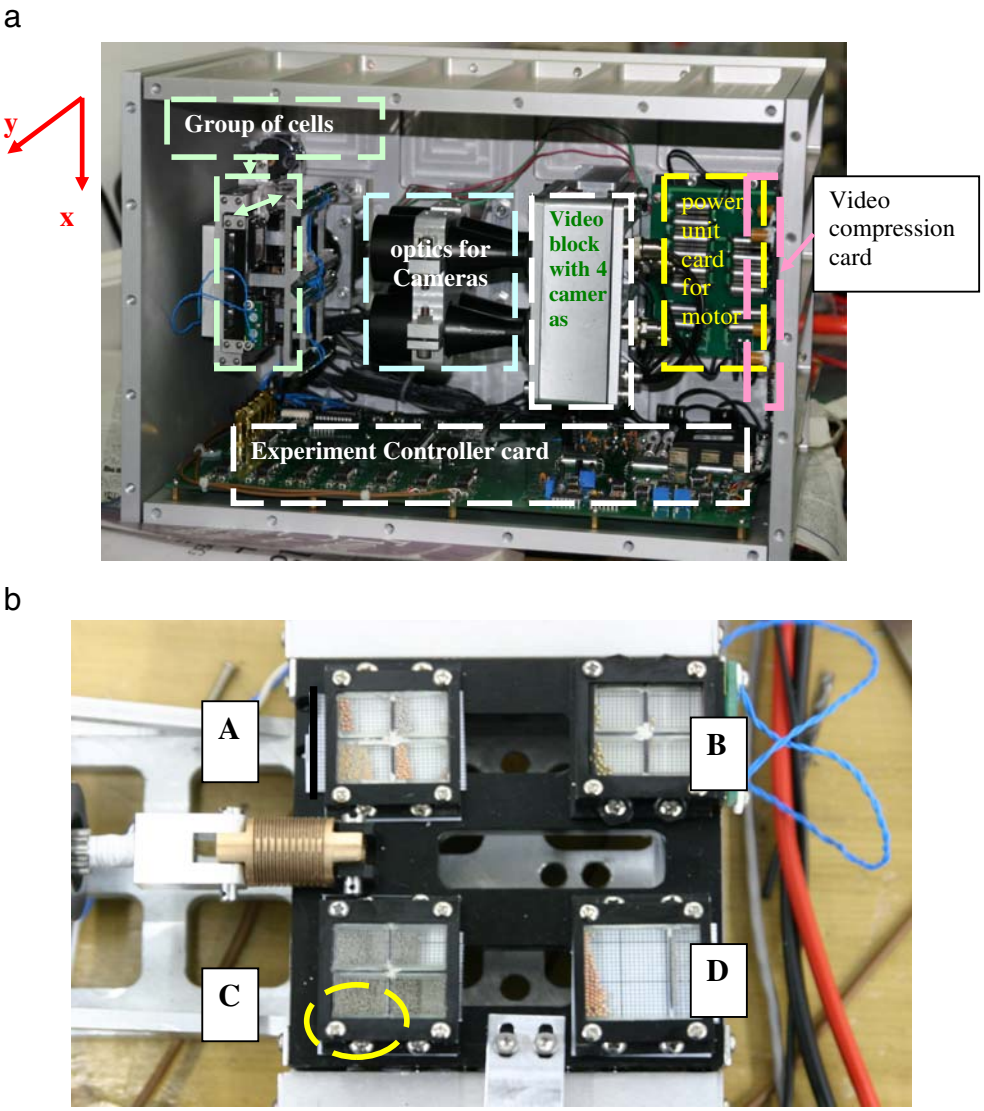

Fig. 1 The setup: (*a*) top view of the apparatus, where one sees the experiment controller card on the bottom, the video compression card on the right hand side, the power unit card for the motor facing front on the right; (*b*) the 14 different cells which are submitted to vibration at the same time. They are divided into 4 groups A, B, C and D, which contain respectively from left to right and top to bottom 2, 4, 4 and 4 cells. Each group is viewed by a single camera. The studied cell is the one with a yellow circle, which is the bottom right cell of the group located on the bottom left group. One sees the motor axis on the right

characteristics (b_k, f_k, T_k,) are listed in Table 1; the experimental accessible range is: $0.02mm < b < 3mm$, $v_b < 15mm/s$, $1.15Hz < f < 10Hz$. After each mode a large-amplitude (3 *mm*) of rapid back-and-forth motion is imposed to reset initial conditions.

As mentioned above, in this paper only data from the cell which contains four moving bronze spheres of diameter (1.21 ± 0.02 *mm*) is concerned. The cell contains also four other bronze balls which are glued to one side of the cell wall (see Fig. 1b). The recorded

Table 1 The vibration amplitude b, frequency f and duration T of each mode and the v_{y_0} obtained from fitting the ball velocity during each mode are given for the 10 vibration modes

Mode	$b(mm)$	$f(Hz)$	$v_b\,(mm/s)$	Duration $T(s)$	$v_{y_0}\,(mm/s)$
1	0.31	1.5	2.94	1261	2.62
2	0.59	1.5	5.58	1263	4.83
3	0.87	1.5	8.22	631	7.77
4	0.4	3	7.54	630	6.74
5	0.59	3	11.16	631	9.94
6	0.70	3	13.27	631	10.42
7	0.77	3	14.48	630	10.00
8	0.19	6	7.24	631	6.17
9	0.38	6	14.48	631	10.45
10	0.22	10	14.07	629	9.88

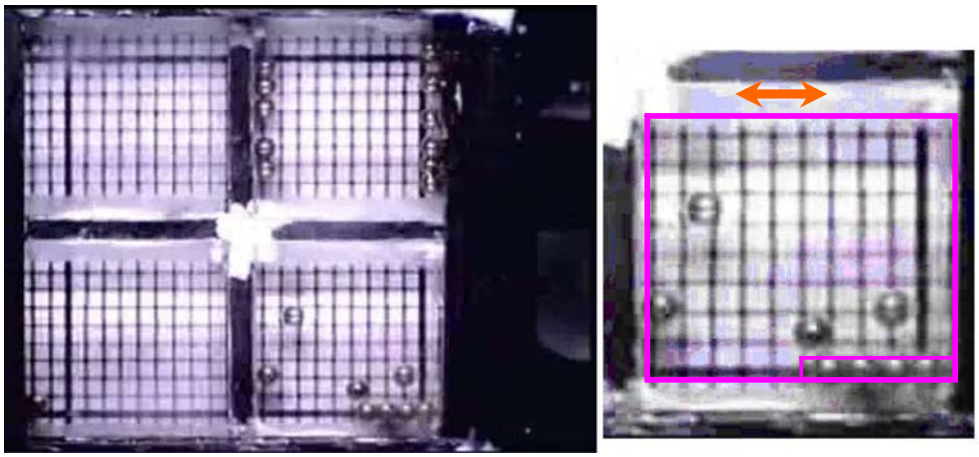

Fig. 2 Left: a snapshot of the 4 cells of group C; right: the moving balls in the studied cell

images in Fig. 2 show that glued particles is on the right part of the bottom wall of the cell. The maximum vibration velocity in each mode ranges from 2.9 *mm/s* to 14.5 *mm/s*. It excites the balls slow enough for a video camera of 25 frames per second to follow the motion of a ball of 1.21 *mm* in size within the cell.

As the frame rate of the camera is rapid compared to the ball speed, position of a ball can be tracked manually at each video image and trajectory of this ball can be determined, in pixel unit. From this, speed of this ball has been determined within an error of the order of 1 *pixel*/*frame*, *i.e.*, 2.8 *mm*/*s*.

Experimental Results

The (x, y) coordinates of the selected ball has been determined frame after frame by manual particle tracking; this allows to plot the trajectory of the ball for the different modes of vibration, and to compute the components v_x, v_y of ball speed in directions perpendicular (x) and parallel (y) to the direction of vibration.

Distributions of particle number density averaged within 5, 10, and 17 minutes using trajectory data in mode 2, as an example, are shown along y direction (top) and x direction (bottom) in Fig. 3. The most likely accessible region in y direction for the ball is from $(2b + r)$ to $(L - r)$ if the farthest location the wall can go to the left is set to be y = 0, where L is the length of the cell, b is the vibration amplitude, and r is the ball radius. There are four glued bronze balls at the left 1 *mm* of the x axis, which cause the lower probability of ball accessing to the area. It can be seen that the ball fills all the possible accessible area in the cell. One can conclude that ball evolves ergodic after a number of collisions since no location is more probable than another within fluctuation.

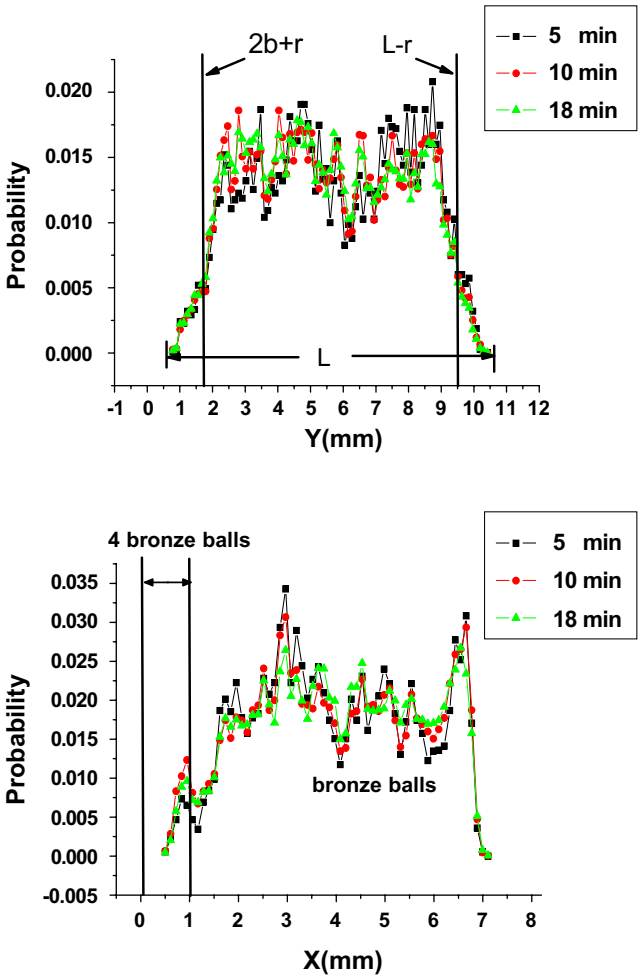

Fig. 3 Ergodicity study using ball trajectory data in mode 2. Distributions of particle number density averaged within 5, 10 and 18 minutes along y direction (top) and x direction (bottom) are plotted, where b is the vibration amplitude along y direction, and r is the ball radius. The farthest location the wall can go to the left is set to be $y = 0$. There are four glued bronze balls at the left 1 *mm* of the x axis, which cause the lower probability of ball accessible to that area. It can be seen that the ball fills all the possible accessible area in the cell

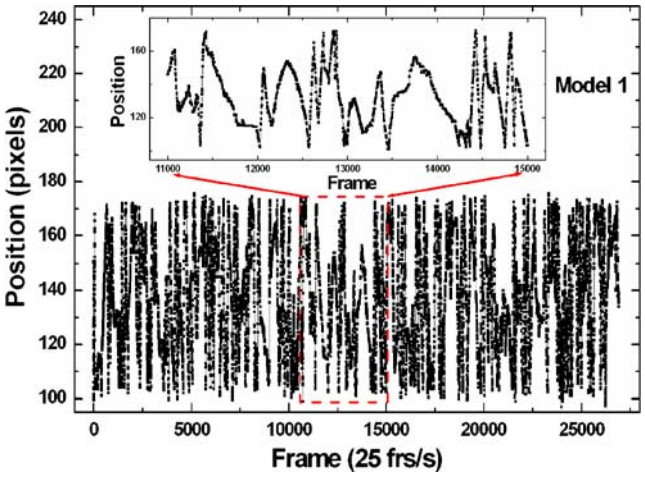

Fig. 4 The trajectory of the ball in mode 1 is traced in (x, y) coordinates in pixel per frame, where y is the direction along the vibration and x is the direction perpendicular to the vibration. In the figure only the traced trajectory of a single ball in y direction is showed as a demonstration

Also as local trajectories are linear, this indicates that the ball goes in the same direction for a few frames (within the experimental uncertainty), then it changes direction. One can ask also whether friction on lateral walls perturbs or dominates the dynamics. A way to study this point is to plot the evolution of the position y of the ball as a function of time since if $y(t)$ is curved it means a progressive change of speed and an influence of the windows, while if y are line segments it indicates that the main evolution of the speed is linked to collisions. An example of the y evolution is given in Fig. 4 for mode 1 excitation, from which one can conclude to the small effect of lateral friction.

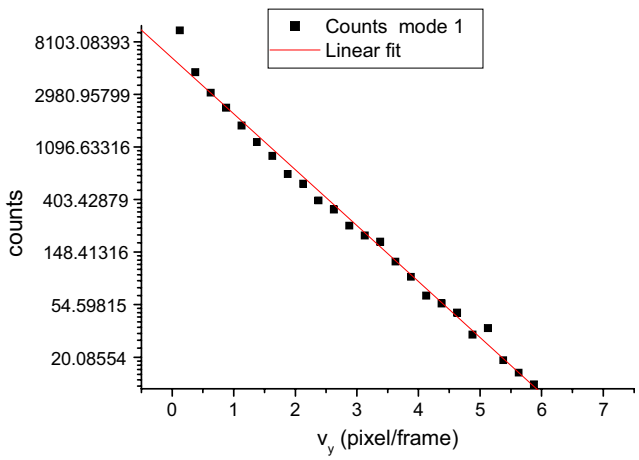

Fig. 5 Velocity distribution in y direction for mode 1 is shown. It can be seen that the distribution is a function of $\exp\left(-\nu_y/\nu_{y_0}\right)$, where ν_{y_0} is a fitting parameter

The probability distribution $\rho(\nu)$ of speed ν can be obtained also from these data: One has just to count the number $N(\nu)$ of how many times the ball has a speed in between ν and $\nu + \delta\nu$, where $\delta\nu$ being fixed, leading to $\rho(\nu)\,\delta\nu = N(\nu)\,\delta\nu/\left[\int N(\nu)\,d\nu\right]$. A typical example is given in Fig. 5 for the component ν_y (component of speed in the direction of vibration) in the case of excitation mode 1. One sees that the distribution is linear in the semi-log plot (with little deviation at small speed), which indicates the distribution is in exponential form. This curve is then characterized by a characteristic speed ν_{y_0}, which is the mean speed of the distribution. Performing the same treatment and analysis for each mode and for both x and y directions, we have found similar exponential trends, with different mean speeds of each component ν_{x_0} and ν_{y_0} for the same mode of excitation; furthermore ν_{y_0} and ν_{x_0} are found to depend on the velocity ν_b. By plotting ν_{y_0} and ν_{x_0} as a function

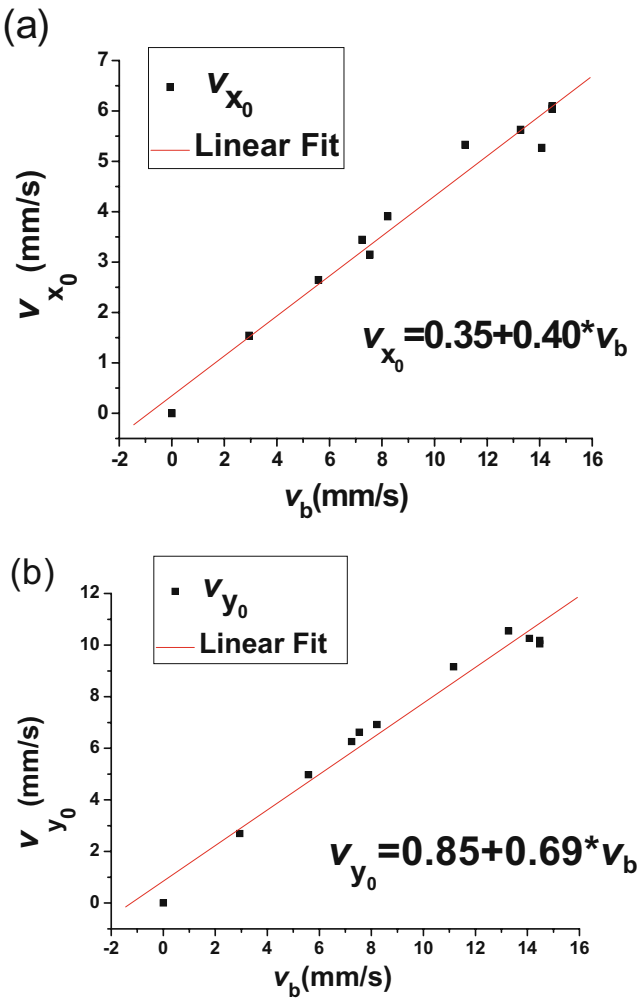

Fig. 6 The characteristic velocities ν_{x_0} and ν_{y_0} versus the vibration velocity $\nu_b = b\omega$: (a) component perpendicular to the vibration direction, (b) component along vibration direction

of v_b, the values are found aligned indicating a linear relationship between v_{x_0}, v_{y_0} and v_b; this is shown in Fig. 6. The relations are found to be:

$$v_{xo}(mm/s) = 0.35(mm/s) + 0.40 \times v_b(mm/s),$$
$$v_{yo}(mm/s) = 0.85(mm/s) + 0.69 \times v_b(mm/s).$$

Since no other parameters can give a speed to the v_{y_0} and v_{x_0}, v_{y_0} and v_{x_0} shall be proportional to v_b. Considering the error due to the image compression is about 2.8 *mm/s*, it is likely that the constants 0.35 *mm/s* and 0.85 *mm/s* come from uncertainty.

As we know now the mean values vary with the mode, we can rescale the distributions and study whether the shape depends on v_b. This is done in Fig. 7a and b for v_x/v_{x_0} and v_y/v_{y_0}, respectively. Curves exhibit a good overlapping that indicates a unique distribution for v_x and v_y. The distribution of v_x looks slightly different from the one for v_y, which is steeper at slow v_y/v_{y_0}, as can be concluded from the slight curvature at small speed which is less pronounced for v_x.

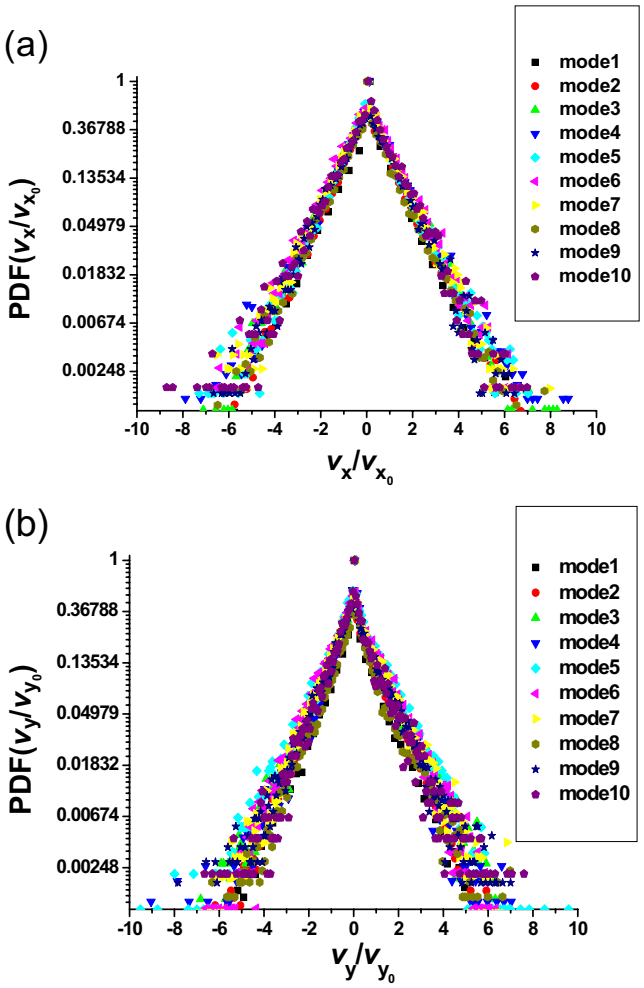

Fig. 7 Probability density functions of (a) (v_x/v_{x_0}) and (b) (v_y/v_{y_0}) in rescaled units. Variations of v_{x_0} and v_{y_0} versus $b\omega$ are given in Fig. 6

At last to confirm the little importance of the solid friction, we have investigated the dependence of the local mean speed in some direction as a function of the location. For instance, if the loss due to friction is large, one should expect a mean speed $v_{y_0}^+(y)$ at $y = b$ when ball is moving towards the direction $+y$ to be larger than the mean speed $v_{y_0}^+(y)$ at $y = L - b$ in the same $+y$ direction, where L is the size of the cell. The difference between the distributions $\rho(v^+, y = b)$ and $\rho(v^+, y = L - b)$ shall give the losses during the travel from b to $L - b$. By averaging the 10 modes the difference of the averaged speed is found to be $(6.8 \pm 1.8)\, mm/s - (6.2 \pm 1.4)\, mm/s$. The losses due to friction on glass windows are inside the error bar and shall be small enough to be accounted for explaining the exponential decrease.

Discussion and Conclusion

It is difficult to perform a direct analysis of the ball dynamics for a few reasons:

Firstly the quality of the compressed image makes automatic tracking difficult that manual tracking is necessary at some point of data processing. The manual tracking introduces some error on the trajectory which makes difficult the determination of the real trajectory and of the speed; for instance, assuming an uncertainty of one pixel, i.e. 0.11 *mm*, leads to an uncertainty δv on the speed v of δv=25 × 0.11 = 2.8 *mm*/s (since the time in between two frames is 0.04 s). It is of the order of the lowest speed v_b used in this experiment.

Secondly, ball-ball collisions and friction on windows can induce rotation of the ball and the combination of both effects can curve the trajectories; but no measurement of the ball rotation can be done, so that the number of free parameters to reconstruct the ball dynamics is too large to allow it to be done safely. This is why it is not possible in this experiment to use collisions as a means to get deeper in the local mechanics which is active during two collisions, nor to use the trajectory to characterize the role of friction on lateral walls. So the only way to analyze the data is through statistical means, which have been determined in the previous section.

In the case of statistical analysis of a gas of particles, an important parameter is the mean free path a particle can perform in between two collisions with other particles. In the present case, the cell size and

the number of balls are small so that one has to take finite-size effects into consideration to calculate l_c. This is done using the effective cell length $L_{eff} = L - d$ instead of L and the effective number of balls N_{eff} which can collide with a given ball, i.e., N_{eff}=(N−1). So l_c satisfies $N_{eff} 2dl_c/(L_{eff})^2 = 1$, which gives $l_c = (L-d)^2/[2d(N-1)]$. Since $N = 4$, $d = 1.21\ mm$, and $L = 10\ mm$, one gets $l_c = 11\ mm = 1.2(L-d)$. As l_c is larger than the effective cell size, the system is in the range of the Knudsen regime, in a situation that particles cannot be considered as only connected to the boundaries, but that they are also weakly coupled.

This situation is analogous to the one which has been studied during Airbus parabolic flights (Falcon et al. 2006; Evesque 2004) with 12 to 48 balls in a fixed cylindrical container with a vibrating piston, where the distribution $p(v)$ of the impacts of balls at speed with a fix gauge has been determined and where it has been found $p(v)$=exp$(-v/v_0)$, which leads in turn to a distribution of speed $\rho(v)$ in the gas bulk varying as $\rho(v) = \left[A/(Sv)\right]\exp(-v/v_0)$ since $p(v)$=$vS\rho(v)$ (where S is the gauge surface). Also, in this previous experiment the speed v_0 has been found to vary as $N^{0.4}$. It seems that both experiments compare relatively well, since they both get an exponential distribution, while they slightly differ due to the $1/v$ pre-factor in the Airbus results. We have no explanation for not getting this pre-factor here; it might be due to little accuracy of the speed measurement at slow speed. However, the curvature of the distribution $\rho(v_y)$ which is observable at low speed in Fig. 6 may result from the existence of this pre-factor. As we could not vary the number of balls during the present experiment we cannot tell whether v_0 varies with N here as it varies with N in the Airbus and with the 3d cell. Also we do not know how v_0 varies with the cell size L at constant l_c/L.

The above results prove that the velocity distribution follows the distribution exp$(-v/v_0)$, which is a non-Boltzmann function, i.e., $\exp\left(-v^2/v_0^2\right)$. Hence they provide another evidence for a "velostat" rather than "thermostat" boundary conditions in dilute granular gas system (Evesque 2004, 2003) in this concentration range. In other words this shape of distribution may probably come from the fact that ball collisions preserve the sum of momenta rather than the sum of kinetic energies (Evesque 2004).

As the 1-ball trajectory covers the whole accessible space after just a few collisions with the boundary, this implies that the system of four balls look already ergodic. This is an important result since it tells that macroscopic quantities can be obtained with such a little system, and can be extrapolated to larger ones. If this is true it may have important consequences on simulation technique. As we know that the single-ball cell experiment does not exhibit the same dynamics and exhibit a strong reduction of the available phase space (Evesque et al. 2005), we conclude that the ergodic nature of the present trajectory results from the numerous ball-ball collisions existing in the present experiment. It is then linked to the value of the mean free path l_c, which is of the order of the cell size L. If l_c is increased largely, keeping L constant, collisions between balls would have become a negligible process, and observation of 1d linear dynamic would have been observed, with periodic motion as in (Leconte et al. 2006a) (if amplitude b would have been large enough). Unfortunately, the single-ball cell experiment, although was programmed in SJ-8 to prove this hypothesis with a 2D cell, did not perform.

At last it is interesting to note that similar exponential trend has been found recently using 2D simulation (Kawarada and Hayakawa 2004) in some other configuration, as soon as one includes solid friction and rotation.

Acknowledgements H. Yang, T. Zhang, and Z. Peng are thanked for their experimental assistance, Z. Yang and Z. Yun are thanked for assistance in data retrieving. CNSF, CAS and CNSA are thanked for the financial support (grant Nos. 10720101074 and KACX2-SW-02–06). PE & YG want to thank CNES & ESA for funding and assistance.

References

Barrat, A., Trizac, E., Ernst, M.H.: Granular gases: dynamics and collective effects, preprint arXiv:cond-mat/0411435 v2, 3/12/2004, to be published in J. Phys. C **17**, S2429 (2005)

Brey, J.J., Ruiz-Montero, M.J.: Velocity distribution of fluidized granular gases in the presence of gravity. Phys. Rev. E. **67**, 021307 (2003)

Evesque, P.: Are temperature and other thermodynamics variables efficient concepts for describing granular gases and/or flows? Poudres & Grains. **13**(2), 20–26 (2003)

Evesque, P.: New corner stones in dissipative granular gases: on some theoretical implication of Liouville's Equation in the physics of loose granular dissipative gases. Poudres & Grains. **14**(2), 8–53 (2004), Mai

Evesque, P., Palencia, F., Lecoutre-Chabot, C., Beysens, D., Garrabos, Y.: Microgravity Sci. Technol. **XVI-1**, 280–284 (2005)

Falcon, E., Wunenburger, R., Evesque, P., Fauve, S., Chabot, C., Garrabos, Y., Beysens, D.: Cluster formation in a granular medium fluidised by vibrations in low gravity. Phys. Rev. Lett. **83**, 440–443 (1999)

Falcon, E., Aumaître, S., Evesque, P., Palencia, F., Lecoutre-Chabot, C., Fauve, S., Beysens, D., Garrabos, Y.: Europhys. Lett. **74**, 830 (2006)

Goldhirsch, I.: Rapid granular flow. Annu. Rev. Fluid Mech. **35**, 267 (2003)

Kawarada, A., Hayakawa, H.: Non-Gaussian velocity distribution function in a vibrating granular bed. J. Phys. Soc. Japan **73**, 2037 (2004)

Leconte, M., Garrabos, Y., Falcon, E., Lecoutre, C., Palencia, F., Evesque, P., Beysens, D.: Journal of statistical mechanics: theory and experiment. P07012 (2006a)
Leconte, M., Garrabos, Y., Palencia, F., Lecoutre, C., Evesque, P., Beysens, D.: Appl. Phys. Lett. **89**, 243518 (2006b)
Losert, W., Cooper, D.G.W., Delour, J., Kudrolli, A., Gollub, J.P.: Velocity statistics in excited granular media. Chaos. **9**, 682 (1999)
McNamara, S., Young, W.R.: Phys. Fluids A. **4**, 496 (1992)
Moon, S.J., Swift, J.B., Swinney, H.L.: Steady-state velocity distributions of an oscillated granular gas. Phys. Rev. E. **69**, 011301 (2004)
Poschel, T., Brilliantov, N.V.: Granular Gas Dynamics, Lectures Notes in Physics, p. 624, Springer, Berlin (2003)
Poschell, T., Luding, S.: Granular gases, Lectures Notes in Physics, p. 564, Springer, Berlin (2001)